LAWRENCE
LIVERMORE
NATIONAL
LABORATORY

UCRL-JRNL-233631

Resonance transition 795-nm Rubidium laser using 3He buffer gas

Sheldon S.Q. Wu, Thomas F. Soules, Ralph H. Page, Scott C. Mitchell, V. Keith Kanz, Raymond J. Beach

August 13, 2007

Optics Communications

Disclaimer

Resonance transition 795-nm Rubidium laser using ^{3}He buffer gas

Sheldon S.Q. Wu,* Thomas F. Soules, Ralph H. Page, Scott C. Mitchell, V. Keith Kanz, Raymond J. Beach

Lawrence Livermore National Laboratory, 7000 East Avenue, Livermore, California 94551

We report the first demonstration of a 795-nm Rubidium resonance transition laser using a buffer gas consisting of pure ^{3}He. This follows our recent demonstration of a hydrocarbon-free 795-nm Rubidium resonance laser which used naturally-occurring He as the buffer gas. Using He gas that is isotopically enriched with ^{3}He yields enhanced mixing of the Rb fine-structure levels. This enables efficient lasing at reduced He buffer gas pressure, improving thermal management in high average power Rb lasers and enhancing the power scaling potential of such systems.

Alkali resonance lasers are being actively investigated as an attractive route for the brightness enhancement, both spatial and spectral, of laser diode arrays. Since the first demonstration of a rubidium optical resonance transition laser in 2002 [1], multiple demonstrations of alkali resonance transition lasers have been reported in the scientific literature using Rb [2, 3], Cs [4, 5, 6] and K [7] as the gain media. All these systems have similar lasing schemes, being pumped on their D_2 transition ($n^2S_{1/2} \rightarrow n^2P_{3/2}$) and lased on their D_1 transition ($n^2P_{1/2} \rightarrow n^2S_{1/2}$). With one exception, all of the published demonstrations have followed Konefal's original suggestion [8] and used ethane as the buffer gas or a component of the buffer gas to promote rapid F-S (fine-

structure) mixing between the terminal pump level ($^2P_{3/2}$) and the initial laser level ($^2P_{1/2}$). Rapid F-S mixing is a requirement for efficient laser operation. The problem with this approach, as first reported by Page et al [2], is that it leads to the deposition of carbon on surfaces that simultaneously see high intensity pump light, alkali vapor and ethane. Due to the high optical absorption of carbon compounds to both the pump and laser light, the deposition of carbon quickly leads to thermally-initiated optical damage. Because we are ultimately interested in using end-pump geometries in which high-intensity pump light is ducted through a cell via reflections with the side walls where pump light, ethane and alkali vapor exist simultaneously, the cell-fouling issue that accompanies the use of ethane requires mitigation, especially for power scaled systems. Wu *et al* recently demonstrated one solution to this problem with a hydrocarbon-free resonance transition 795-nm Rubidium laser in which the buffer gas was naturally-occurring He (natural abundance of ^{3}He: ^{4}He is ~1:740000) [3]. In that work, the good agreement between measured laser performance and a laser model supported the clean He-only buffer gas approach as a viable path for power scaling. Obviated was the issue of carbon formation and degradation of the vapor cell that is observed when ethane is used as a component of the buffer. One potential disadvantage of the pure He buffer gas approach arises from the smaller F-S mixing cross section of Rb-He, reported to be 4.6×10^{-17} cm^2 based on laser model-fit [3], compared to that of Rb-ethane, reported to be 7.7×10^{-15} cm^2 [9]. The impact of these differing cross section values means that to achieve equivalent F-S mixing rates, higher pressures are required in the pure He systems than would be required in systems using ethane as a buffer gas component. The primary disadvantage of higher He pressures for power scaled systems is that the refractive index variation with temperature dn/dT in the alkali gain cell is proportional to the He pressure, so higher He pressures will give larger thermal aberrations under equivalent

heat loads. In this letter, we demonstrate one approach to lowering the required He pressure in the alkali vapor gain cell by replacing the He buffer gas having a natural isotopic abundance with isotopically enriched ^{3}He.

The advantage of using isotopically enriched ^{3}He stems from its lower mass and therefore higher thermal speed at a given temperature in comparison with naturally occurring He. The higher thermal speed associated with ^{3}He benefits the F-S mixing rate, $\gamma_{^2P_{3/2}\rightarrow{}^2P_{1/2}} = n_{He}\sigma_{^2P_{3/2}\rightarrow{}^2P_{1/2}}v_r$, where n_{He} is the number of He atoms per unit volume, $\sigma_{^2P_{3/2}\rightarrow{}^2P_{1/2}}$ is the Rb-He F-S mixing cross section, and v_r is the mean relative speed between He and Rb atoms. First, at a given temperature v_r is higher in ^{3}He than ^{4}He by approximately $\sqrt{4/3} \approx 1.15$, which not only benefits the F-S mixing rate which depends directly on v_r, but also improves thermal management in the cell. Since the thermal conductivity of an ideal gas is proportional to the mean particle velocity, the thermal conductivity of ^{3}He is larger than that of ^{4}He by the same factor. Secondly, the F-S mixing cross section itself has a velocity dependence [10] that is expected to give a Rb-^{3}He value larger than the Rb-^{4}He value at a given cell temperature due to the difference in thermal speeds of the two He isotopes. It can be extrapolated from that velocity dependence that the Rb F-S mixing cross section in ^{3}He is approximately 1.5 times larger than that of ^{4}He at our operating temperatures. Together, one can expect a Rb F-S mixing rate about 1.7 times larger for the ^{3}He system than the ^{4}He system under same operating conditions. A summary of significant parameters is provided in Table 1.

A schematic diagram for the experimental setup used in this demonstration that is nearly identical to that of [3] is shown in Figure 1. The Rb vapor and ^{3}He gas were contained in a 3 cm long cylindrical ceramic cell with misoriented sapphire windows that were anti-reflection coated on their external surfaces, but uncoated on their internal surfaces. Rb was introduced into the

cell as a pure metal. This was followed by cell evacuation using a laboratory vacuum system followed by the introduction of 40 psi of ^{3}He gas (2.7 atm) at room temperature (~20°C). The ^{3}He gas is manufactured by Spectra Gases Inc. with a quoted 99.999% chemical purity and 99.9% isotopic enrichment. The cell was placed in a close-fit copper oven with electric heaters that allowed us to maintain the cell temperature to within 1°C and fix the resulting Rb saturated vapor pressure inside the cell.

The pump source used was a Ti:sapphire laser that produced up to 2.4 W of linearly polarized, near-diffraction-limited CW optical radiation. The Ti:sapphire laser linewidth was ~9 GHz FWHM making the pump laser source narrow compared to the He-broadened D_2 pump absorption feature, which we estimate is ~50 GHz wide based on the known Rb-^{3}He collisional broadening rate of 20.8 GHz/amagat [11, 12]. The pump light was coupled into the 41.5 cm physical length laser cavity via a polarizing beam splitter and traversed the vapor cell twice by reflecting off the highly reflecting end mirror. Stable cavity mode is formed with aid from gain guiding due to the nonuniform transverse gain profile over the length of our cell. The end mirror has a reflectivity of 0.99 at both the pump and lasing wavelengths. The pump beam was aligned parallel to the laser cavity axis and focused to a 220 μm diameter spot size at the center of the cell, resulting in peak pump irradiance of nearly 5 kW/cm^2. Since the optic axes of the pair of sapphire windows were soldered onto the cell at unknown orientations, a half-wave plate was placed in the cavity to partially compensate for the polarization changes caused by birefringence. We estimate that even with the half-wave plate, laser light traversing the cell had a 75% transmission efficiency passing the cube polarizer on its return path. Coupled with the uncoated window surfaces, the single-pass passive optical loss is close to 40% in our laser cavity.

Laser emission at 795 nm in a TEM_{00} beam was observed at cell temperatures in the vicinity of 145°C. Maximum output powers of over 350 mW were measured, corresponding to an optical-optical efficiency greater than 21%. Large cavity losses along with the high gains that characterize alkali atoms place the optimal output coupler reflectivity below 0.2. Presented in Figure 2 is the theoretical and measured laser output power versus pump power using different output couplers at a cell temperature of 142°C. The theoretical curves overlaying the experimental data points were calculated using a laser model previously developed by Beach *et al* [4]. Because of the larger Rb-^{3}He collision cross section compared to that of ^{4}He, the mixing rate between the F-S levels is high enough to maintain efficient lasing at these pump levels. The saturation effect observed in [3] for the Rb-^{4}He laser in which the slope efficiency decreased at higher pump powers due to insufficient F-S mixing is significantly diminished here with nearly identical operating conditions, supporting the use of ^{3}He with its larger F-S mixing rate for power scaled systems. Treating the Rb-^{3}He F-S mixing rate and the mode overlap efficiency as adjustable parameters, the model curves were generated using an effective Rb-^{3}He F-S mixing cross section value of 7.1×10^{-17} cm^2 and 57% mode overlap efficiency. Mode overlap is defined in [4] as the fraction of the pump excited volume in the alkali cell extracted by the circulating laser radiation in the resonator. We note the Rb-^{3}He fine-structure mixing rate that gives the best fit between our model and experimental data is approximately 1.5 times larger than our experimentally fitted value for the Rb-^{4}He cross section reported in [3].

In conclusion, we have demonstrated the operation of a 795-nm Rubidium resonance laser system using a buffer gas consisting of pure ^{3}He. The use of pure He for the buffer gas, either natural abundance or isotopically enriched ^{3}He, as opposed to the more common approach to date of using a hydrocarbon containing buffer gas should enable high reliability Rb based

diode-pumped alkali laser (DPAL) systems by eliminating the carbon deposition problem in the laser cells that occurs with the hydrocarbon approach [2]. For our pure He buffer gas approach, the use of isotopically enriched ^{3}He offers multiple advantages over the use of naturally occurring He. The higher thermal velocity of ^{3}He than that of ^{4}He give a Rb F-S mixing rate about 1.7 times larger for the ^{3}He system than the ^{4}He system under the same operating conditions. This higher F-S mixing rate, which is critical for efficient laser performance, enables comparable performing ^{3}He systems at only 58% of the He buffer gas pressure required for the ^{4}He systems. Since thermal aberrations in the laser's Rb vapor cell are governed by dn/dT which is proportional to the He pressure, the ^{3}He approach will be advantageous for high beam quality lasers in power scaled systems [4]. Another benefit of ^{3}He based systems over ^{4}He based systems is the higher thermal conductivity κ of ^{3}He, $\kappa_{^3He} : \kappa_{^4He} \sim 1.15 : 1$ -- an important consideration in thermal management driven designs of power scaled systems. In view of these advantages of ^{3}He over ^{4}He based systems, we expect the ^{3}He approach to be the preferred route to power scaling DPAL lasers to efficient, reliable, and good beam quality systems. Due to their projected efficiency advantages over diode-pumped solid state lasers (DPSSLs), their compatibility with commercially available laser diode arrays, and now a demonstrated system that promise very high reliability, diode-pumped ^{3}He-only Rb lasers will potentially compete favorably with DPSSLs in many applications that require high beam quality CW or quasi-CW laser operation.

We are grateful to Professor Paul Yu of UC San Diego; John O'Pray, Mike Tobin, Kevin Zondervan, Jim Kotora, Denise Podolski and Mark Rotter all of the Missile Defense Agency; and Chris Barty of Lawrence Livermore National Laboratory for their support and many useful discussions. We also gratefully acknowledge the financial support provided by the Missile

Defense Agency. This work was performed under the auspices of the U.S. DOE, by UC, LLNL under Contract W-7405-ENG-48.

*Also with the Department of Electrical and Computer Engineering, University of California at San Diego, La Jolla, California 92093-0407.

Table 1. Important physical parameters for Rb laser performance. λ_{MFP} denotes the mean free path. Other symbols have their usual meaning.

Physical Parameter	Expression	Value for ^{3}He / Value for ^{4}He
Mean particle velocity	$v_r = \sqrt{\frac{8}{\pi}\frac{k_B T}{\mu}} \approx \sqrt{\frac{8}{\pi}\frac{k_B T}{m_{He}}}$	$\sqrt{4/3}$
Rb-He fine-structure mixing cross section	$\sigma_{^2P_{3/2}\rightarrow{}^2P_{1/2}}$ (experimentally determined [10])	1.5 at T=142°C
Fine-structure mixing rate	$\gamma_{^2P_{3/2}\rightarrow{}^2P_{1/2}} = n_{He}\sigma_{^2P_{3/2}\rightarrow{}^2P_{1/2}} v_r$	1.7
Thermal conductivity	$\kappa = n_{He} v_r \lambda_{MFP} k_B / 2$	$\sqrt{4/3}$
Collisional broadening rate of Rb D_2 line	(experimentally determined [12])	1.15

Figure 1

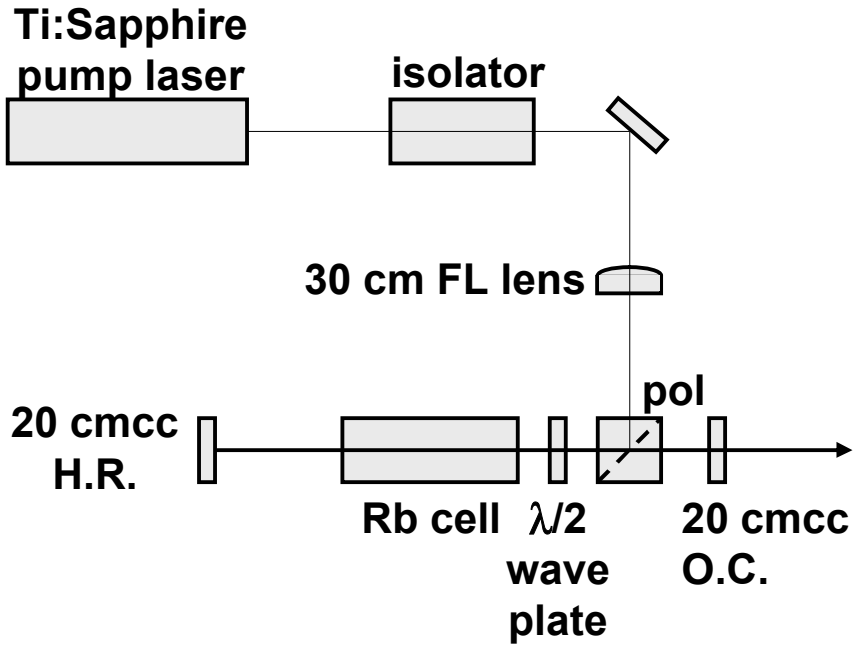
Ti:Sapphire
pump laser
isolator
30 cm FL lens
pol
20 cmcc
H.R.
Rb cell
λ/2
wave
plate
20 cmcc
O.C.

Figure 2

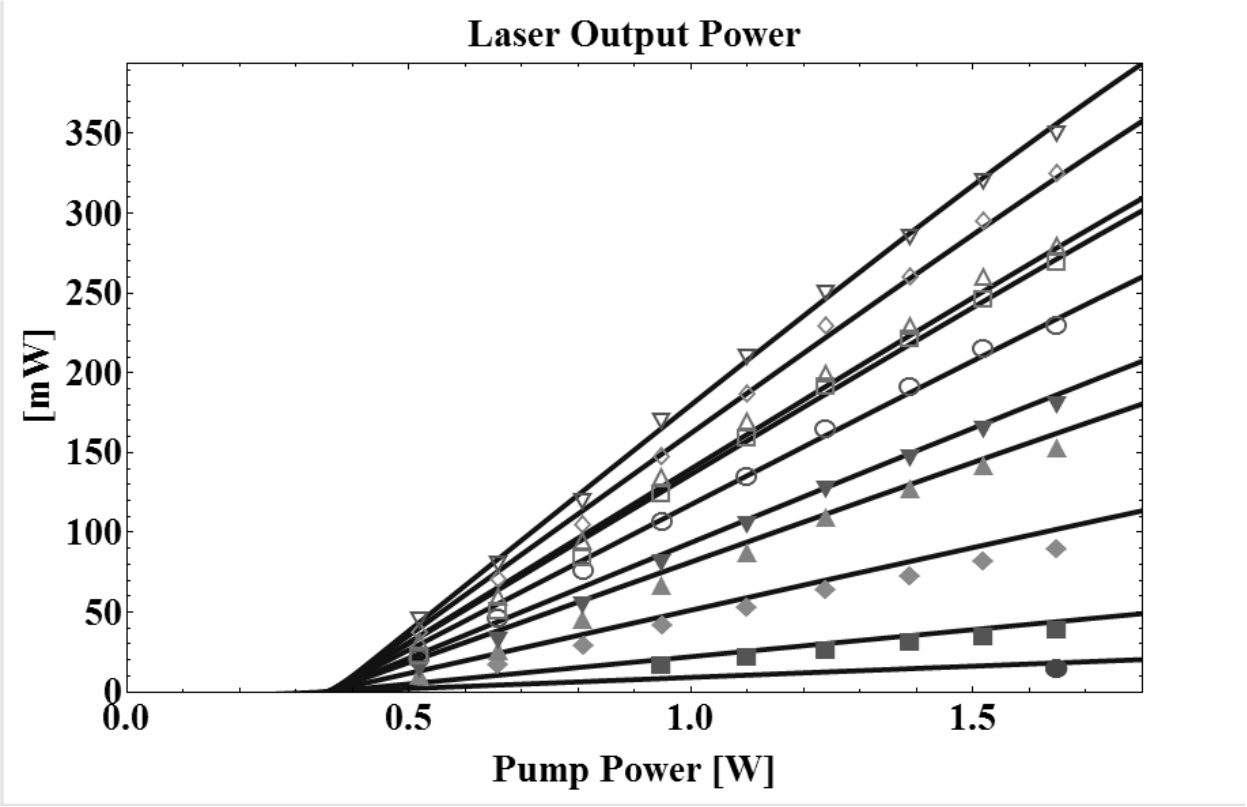
Laser Output Power
350
300
250
200
150
100
50
0
[mW]
0.0
0.5
1.0
1.5
Pump Power [W]

Figure Captions

Fig. 1. Schematic diagram of the experimental setup used in our demonstrations. The laser cavity mirrors have ~20 cm radii of curvature and are both concave (cc). H.R. stands for high reflector, O.C. for output coupler and FL for focal length. The Rb cell is enclosed in a copper oven and heated to the operating temperature of 142°C.

Fig. 2. Rb laser output power for various output couplers plotted against pump power. Solid curves represent model predictions. From top to bottom, the reflectivities are: 0.19, 0.32, 0.46, 0.48, 0.58, 0.69, 0.74, 0.85, 0.94 and 0.976. The reflectivities were directly measured using a Ti:sapphire probe beam at 795 nm.

References

1. W. F. Krupke, R. J. Beach, V. K. Kanz, and S. A. Payne,‘‘Resonance transition 795-nm rubidium laser,’’ Opt. Lett. 28, 2336–2338 (2003).

2. R. H. Page, R. J. Beach, V. K. Kanz, and W. F. Krupke, "Multimode-diode-pumped gas (alkali-vapor) laser," Opt. Lett. 31, 353-355 (2006).

3. S. S.Q. Wu, T. F. Soules, R. H. Page, S. C. Mitchell, V. K. Kanz, R. J. Beach, “Hydrocarbon-free resonance transition 795-nm Rubidium laser,” Accepted for publication in Optics Letters.

4. R. J. Beach, W. F. Krupke, V. K. Kanz, S. A. Payne, M. A. Dubinskii, and L. O. Merkle, "End-pumped continuous-wave alkali vapor lasers: experiment, model, and power scaling," J. Opt. Soc. Am. B 21, 2151-2163 (2004).

5. T. Ehrenreich, B. Zhdanov, T. Takekoshi, S. P. Phipps, and R. J. Knize, ”Diode Pumped Cesium Laser”, Electronics Lett. 41, 47-48 (2005).

6. Y. Wang, T. Kasamatsu, Y. Zheng, H. Miyajima, H. Fukuoka, S. Matsuoka, M.Niigaki, H. Kubomura, T. Hiruma, H. Kan, “ Cesium vapor laser pumped by a volume-Bragg-grating coupled quasi-continuous-wave laser-diode array”, Appl. Phys. Lett. 88, 141112 (2006).

7. B. Zhdanov, C. Maes, T. Ehrenreich, A. Havko, N. Koval, T. Meeker, B. Worker, B. Flusche and R. J. Knize, “Optically Pumped Potassium Laser”, Opt. Com. 270, 353-355 (2007).

8. Z. Konefal, “Observation of collision induced processes in rubidium-ethane vapour”, Opt. Com. 164, 95-105 (1999).

9. E. S. Hrycyshyn and L. Krause, ‘‘Inelastic collisions between excited alkali atoms and molecules. VII. Sensitized fluorescence and quenching in mixtures of rubidium with H2, HD, D2, N2, CH4 , CD4 , C2H4 , and C2H6,’’ Can. J. Phys. 48, 2761–2768 (1970).

10. A. Gallagher, “Rubidium and Cesium Excitation Transfer in Nearly Adiabatic Collisions with Inert Gases”, Phys. Rev. 172, 88 (1968).

11. A. Andalkar and R. B. Warrington, “High-resolution measurement of the pressure broadening and shift of the Cs D_1 and D_2 lines by N_2 and He buffer gases”, Phys. Rev. A 65, 032708 (2002).

12. M. V. Romalis, E. Miron, and G. D. Gates, “Pressure broadening of Rb D_1 and D_2 lines by ^{3}He, ^{4}He, N_2, and Xe: Line cores and near wings”, Phys. Rev. A 56, 4569–4578 (1997).